

International Journal of Hydrogen Energy

Cushion Gas Effects on Hydrogen Storage in Porous Rocks: Insights from Reservoir Simulation and Deep Learning

--Manuscript Draft--

Manuscript Number:	
Article Type:	Full Length Article
Section/Category:	Hydrides / Hydrogen Storage
Keywords:	Underground hydrogen storage, Cushion gas, Porous rocks, Reservoir simulation, Machine learning
Corresponding Author:	Mohamed Mehana Los Alamos National Laboratory UNITED STATES
First Author:	Shaowen Mao, Ph.D.
Order of Authors:	Shaowen Mao, Ph.D. Bailian Chen, Ph.D. Misael Morales Mohamed Malki Mohamed Mehana
Abstract:	Underground hydrogen (H ₂) storage (UHS) is crucial for the H ₂ economy, offering scalable and long-term solutions vital for reliable and sustainable H ₂ -based energy systems. Cushion gas is a common component in UHS designs, but its impact on H ₂ storage performance is not yet fully understood. This study systematically investigates cushion gas effects on H ₂ storage in porous rocks, specifically saline aquifers and depleted gas reservoirs, using reservoir simulations and deep learning. Firstly, we conducted 8000 reservoir simulations for UHS operations in two types of storage formations, considering four cushion gas scenarios: no cushion gas, methane (CH ₄), nitrogen (N ₂), and carbon dioxide (CO ₂). These simulations cover a wide range of geological and operational parameters relevant to practical UHS projects. From these simulations, we derived key insights into the physical mechanisms governing UHS processes and proposed critical storage performance metrics including H ₂ withdrawal efficiency, produced H ₂ purity, produced gas-water ratio, and well injectivity. Then, we developed a unified reduced-order model (ROM) using deep learning based on the comprehensive simulation results. The ROM accurately predicts the cyclic evolution of performance metrics and is over 5,000,000 times faster than traditional physics-based simulations, allowing for thorough uncertainty quantification of UHS performance prediction under various geological and operational conditions. Key findings of this study include: (a) UHS in porous rocks is technically promising, with improving storage performance over cycles; (b) UHS in saline aquifers has higher withdrawal efficiency and purity but lower gas-water ratio and injectivity compared to depleted gas reservoirs; (c) In saline aquifers, cushion gas reduces withdrawal efficiency and purity but significantly enhances gas-water ratio and injectivity, making it particularly beneficial in scenarios with high water production risks; (d) In depleted gas reservoirs, cushion gas is less important under the current operational conditions, as it barely affects withdrawal efficiency and purity, and these reservoirs inherently exhibit high gas-water ratio and injectivity due to initial/leftover native gas (mostly CH ₄); (e) The cushion gas type slightly affects storage performance, with N ₂ slightly outperforming CH ₄ and CO ₂ in withdrawal efficiency and purity, CO ₂ being better for gas-water ratio, and CH ₄ for injectivity. The results of this study support cushion gas designs in future UHS projects in saline aquifers and depleted gas reservoirs.



Los Alamos National Laboratory
 P.O. Box 1663
 Los Alamos, NM 87545
 505- 570-9380

Earth and Environmental Sciences Division

Date: February 3, 2024

Dear Editors of *International Journal of Hydrogen Energy*:

We wish to submit an article entitled "**Cushion Gas Effects on Hydrogen Storage in Porous Rocks: Insights from Reservoir Simulation and Deep Learning**" for consideration in *International Journal of Hydrogen Energy*. We confirm this work is original and has not been published elsewhere, nor is it currently considered for publication elsewhere. Cushion gas is an important component in underground hydrogen (H_2) storage (UHS). However, the cushion gas effects on H_2 storage performance are not fully understood. This paper systematically investigates cushion gas effects on UHS in porous rocks, particularly saline aquifers, and depleted gas reservoirs, for the first time through reservoir simulations and deep learning. Initially, we conducted 8000 reservoir simulations for UHS operations in these formations, considering four cushion gas scenarios: none, CH_4 , N_2 , and CO_2 . The results from these simulations not only provide insights into the governing physics of UHS processes but also create datasets for developing a reduced-order model (ROM). Building on this extensive simulation data, we developed a robust ROM, significantly faster - over 5,000,000 times - than the physics-based simulations. The ROM's efficiency enables extensive uncertainty quantification in UHS performance prediction and systematic evaluation of cushion gas effects in these rocks. The findings of this study offer valuable support for cushion gas designs in future UHS projects in saline aquifers and depleted gas reservoirs.

We elected the *International Journal of Hydrogen Energy* to publish this manuscript since the work aligns well with the Journal's aim and scope on environmentally sustainable exploration, storage, and utilization of H_2 sources to support energy transition and net-zero carbon goal. Our goal is to provide the energy transition pathway from fossil fuels to H_2 energy to decarbonize the economy and create an environmentally sustainable future.

We have no conflicts of interest to disclose. We appreciate your time and effort in reviewing our work. Please address all correspondence concerning this manuscript to Mohamed Mehana at mzm@lanl.gov. Thank you for your consideration of this manuscript. We look forward to hearing from you.

Sincerely,

Mohamed Mehana
 Digitally signed by Mohamed
 Mehana
 Date: 2024.02.03 15:31:59 -07'00'

Mohamed Mehana
 Scientist
 Energy and Natural Resources Security Group (EES-16)
 Los Alamos National Laboratory lanl.gov

Suggested Reviewers

Shihao Wang, Ph.D.

Lead Research Scientist, Chevron Inc

shihao.wang@chevron.com

Dr. Wang is the lead research scientist in Chevron. He has extensive experience with subsurface research, including hydrocarbon development, carbon sequestration, and underground hydrogen storage.

Sahar Bakhshian, Ph.D.

Research Scientist, University of Texas at Austin Bureau of Economic Geology

sahar.bakhshian@beg.utexas.edu

Dr. Bakhshian has extensive research experience in subsurface science and engineering, including hydrocarbon development, CO₂ sequestration, and underground hydrogen storage.

Soheil Saraji, Ph.D.

Assistant Professor, University of Wyoming

ssaraji@uwyo.edu

Dr. Saraji is an associate professor in Energy & Petroleum Engineering, adjunct Professor at School of Energy Resources. He is an expert in CO₂ sequestration and underground hydrogen storage. He has published many important papers about subsurface research.

Yongqiang Chen, Ph.D.

Research Scientist, CSIRO

Yongqiang.chen@csiro.au

Dr. Chen has extensive research experience in subsurface science and engineering. He publishes many excellent papers about CO₂ sequestration and hydrogen storage.

Research highlights:

- Performed extensive three-dimensional compositional reservoir simulations for underground hydrogen storage (UHS) in saline aquifers and depleted gas reservoirs under four cushion gas scenarios: none, CH₄, N₂, and CO₂, incorporating a wide range of geological and operational parameters.
- Proposed four critical UHS performance metrics to quantitatively evaluate the storage performance: H₂ withdrawal efficiency, produced H₂ purity, produced gas-water ratio, and well injectivity.
- Developed an accurate reduced-order model (ROM) based on the reservoir simulation data leveraging deep learning. The ROM is over 5,000,000 times faster than physics-based reservoir simulation.
- Utilized the ROM for comprehensive uncertainty quantification in UHS performance prediction and conducted system-level analysis on the cushion gas effects on storage performance.

Overall, this study for the first time systematically investigated cushion gas effects on underground hydrogen storage performance in both saline aquifers and depleted gas reservoirs. The system-level study not only leverages three-dimensional compositional reservoir simulation but also deep learning techniques. The results of this study can offer valuable guidance to the cushion gas designs in future underground hydrogen storage projects, thus benefiting energy transition and hydrogen economy.

Cushion Gas Effects on Hydrogen Storage in Porous Rocks: Insights from Reservoir Simulation and Deep Learning

Shaowen Mao*, Bailian Chen, Misael Morales, Mohamed Malki, Mohamed Mehana*

Earth and Environmental Sciences Division, Los Alamos National Laboratory, Los Alamos, New Mexico
87545, United States. *Corresponding author; email: shaowen.mao@lanl.gov, mzm@lanl.gov

Abstract

Underground hydrogen (H_2) storage (UHS) is crucial for the H_2 economy, offering scalable and long-term solutions vital for reliable and sustainable H_2 -based energy systems. Cushion gas is a common component in UHS designs, but its impact on H_2 storage performance is not yet fully understood. This study systematically investigates cushion gas effects on H_2 storage in porous rocks, specifically saline aquifers and depleted gas reservoirs, using reservoir simulations and deep learning. Firstly, we conducted 8000 reservoir simulations for UHS operations in two types of storage formations, considering four cushion gas scenarios: no cushion gas, methane (CH_4), nitrogen (N_2), and carbon dioxide (CO_2). These simulations cover a wide range of geological and operational parameters relevant to practical UHS projects. From these simulations, we derived key insights into the physical mechanisms governing UHS processes and proposed critical storage performance metrics including H_2 withdrawal efficiency, produced H_2 purity, produced gas-water ratio, and well injectivity. Then, we developed a unified reduced-order model (ROM) using deep learning based on the comprehensive simulation results. The ROM accurately predicts the cyclic evolution of performance metrics and is over 5,000,000 times faster than traditional physics-based simulations, allowing for thorough uncertainty quantification of UHS performance prediction under various geological and operational conditions. Key findings of this study include: (a) UHS in porous rocks is technically promising, with improving storage performance over cycles; (b) UHS in saline aquifers has higher withdrawal efficiency and purity but lower gas-water ratio and injectivity compared to depleted gas reservoirs; (c) In saline aquifers, cushion gas reduces withdrawal efficiency and purity but significantly enhances gas-water ratio and injectivity, making it particularly beneficial in scenarios with high water production risks; (d) In depleted gas reservoirs, cushion gas is less important under the current operational conditions, as it barely affects withdrawal efficiency and purity, and these reservoirs inherently exhibit high gas-water ratio and injectivity due to initial/leftover native gas (mostly CH_4); (e) The cushion gas type slightly affects storage performance, with N_2 slightly outperforming CH_4 and CO_2 in withdrawal efficiency and purity, CO_2 being better for gas-water ratio, and CH_4 for injectivity. The results of this study support cushion gas designs in future UHS projects in saline aquifers and depleted gas reservoirs.

1 Introduction

Hydrogen (H_2) is rapidly gaining recognition as a low-carbon fuel option for transportation, electricity generation, manufacturing applications, and clean energy technologies, playing a crucial role in advancing the transition to a low-carbon economy [1, 2]. However, the safe and effective storage of H_2 at scale remains a significant challenge [3, 4]. In response, underground H_2 storage (UHS) emerges as a promising solution, leveraging the ample storage capacities of geological formations [3–5]. Potential formations for UHS include salt caverns [6–9], saline aquifers [10–14], and depleted gas reservoirs [15–19]. Currently, practical UHS experience is limited to salt caverns, and the UHS in porous rocks (saline aquifers and depleted gas reservoirs) is still waiting for pilots and demonstration projects [4]. Compared to salt caverns, porous rocks offer considerably greater storage capacity and are more geographically abundant to enable H_2 economy [20]. Therefore, it is critical to explore storage opportunities in porous rocks.

UHS in porous rocks presents significant uncertainties in storage performance due to complicated geological and operational conditions [21]. The operational complexity arises not only from the cyclical nature of UHS operations but also from the injection of cushion gas. Cushion gas is the base gas injected into the formation before H_2 cycling to maintain adequate pressure and deliverability rates during H_2 withdrawal stages. Typical cushion gases include methane (CH_4), nitrogen (N_2), and carbon dioxide (CO_2) [22–30]. Understanding cushion gas effects on storage performance is vital for designing effective UHS projects.

Much research has been conducted to investigate the impact of cushion gas on UHS performance in porous rocks, both experimentally [31–34] and numerically [16, 17, 22–30]. Most of the research relies on computational modeling, as detailed in Table 1. These studies have examined the impact of cushion gas in various storage formations, including saline aquifers, depleted gas reservoirs, depleted oil reservoirs, and gas condensate reservoirs. While providing valuable insights into UHS processes, these studies also reveal certain limitations. Firstly, most previous studies focus on a single set of geological and operational conditions in their numerical simulations. Therefore, the observations and conclusions derived from a specific geological formation or storage strategy may not be easily generalized to UHS projects under diverse geological and operational circumstances. Secondly, previous research often overlooks certain crucial UHS performance metrics. While H_2 withdrawal/recovery efficiency and purity are frequently analyzed, key metrics associated with water production and well injectivity have received less attention. Thirdly, no comparative study has been conducted to systematically investigate the cushion gas effects on H_2 storage performance across different porous rocks. Since cushion gas effects can vary significantly among different storage formations, it is crucial to evaluate them for each specific formation. The lack of comprehensive, system-level studies is largely due to the high computational cost of multi-physics simulations. Conducting extensive reservoir

Literature	Reservoir	Cushion Gas	Performance Metric	Conclusion
[22]	Saline aquifer	N ₂	Production rate, H ₂ purity, water production	N ₂ increases reservoir pressure
[23]	Saline aquifer	Not specified	H ₂ injection/production rate, water production	Cushion gas affects H ₂ injectivity, productivity, and storage capacity
[30]	Saline aquifer	CH ₄ , CO ₂	H ₂ recovery, purity	CH ₄ for higher purity, CO ₂ for higher recovery
[24]	Saline aquifer	N ₂ , CO ₂	H ₂ recovery	N ₂ for higher recovery
[25]	Saline aquifer	CH ₄ , CO ₂ , N ₂	Reservoir pressure, H ₂ purity, production rate	CH ₄ and N ₂ maintain pressure, CO ₂ for purity
[26]	Saline aquifer	CH ₄ , CO ₂ , N ₂	H ₂ recovery, purity, storage capacity	CO ₂ for capacity, CH ₄ for recovery
[16, 17]	Depleted gas reservoir	CO ₂ , N ₂	Reservoir pressure, gas saturation, purity	N ₂ for higher recovery and purity
[27]	Depleted oil reservoir	CH ₄ , CO ₂ , N ₂	Reservoir pressure, H ₂ recovery	CH ₄ for higher recovery
[28]	Depleted gas condensate reservoir	CH ₄ , CO ₂ , N ₂	Reservoir pressure, H ₂ recovery	N ₂ for better pressure support
[29]	Depleted shale gas reservoir	CO ₂	H ₂ recovery	CO ₂ for higher recovery

Table 1: Numerical studies about cushion gas effects on UHS performance in porous rocks.

simulations for UHS operations in saline aquifers and depleted gas reservoirs, under various cushion gas scenarios, is computationally intensive.

The current work, for the first time, systematically studies the cushion gas effects on H₂ storage performance in porous rocks by integrating reservoir simulation and deep learning. Firstly, we conducted 8,000 simulations for UHS in saline aquifers and depleted gas reservoirs under four cushion gas scenarios: no cushion gas, CH₄, N₂, and CO₂. These physics-based simulations, incorporating a wide range of geological and operational parameters relevant to practical UHS projects, yield insights into the governing physics of UHS processes and enable the prediction of key performance metrics. We proposed four UHS metrics for the quantitative evaluation of storage performance: H₂ withdrawal efficiency (E_h), produced H₂ purity (P_h), produced gas-water ratio (GWR), and well injectivity (J). Secondly, we developed a unified reduced-order

model (ROM) using deep learning based on the comprehensive simulation results. The ROM can accurately predict the cyclic evolution of four metrics and achieve a speedup of over 5,000,000 times compared to physics-based simulations. The ROM's computational efficiency allows for extensive uncertainty quantification with 70,656 realizations, exploring a wide range of input variations. These uncertainty quantification results enable us to grasp the probabilistic nature of UHS performance prediction and systematically evaluate cushion gas effects across two types of storage formations.

The paper is organized as follows: Section 2 outlines the methodology of reservoir simulation and ROM development. Section 3 presents the results of the study, including correlation coefficient analysis, reservoir simulation analysis, ROM performance evaluation, and uncertainty quantification. Section 4 concludes the paper.

2 Methodology

2.1 Reservoir Simulation

We perform three-dimensional (3D) multiphase, compositional reservoir simulations for UHS operations in both saline aquifers and depleted gas reservoirs under different cushion gas scenarios. These simulations are executed using the tNavigator [35] and are run on servers within the Earth and Environmental Sciences Division at Los Alamos National Laboratory. This section summarizes the setup and parameters of these numerical simulations.

The assumptions of reservoir simulations include: (a) The reservoirs are homogeneous and isotropic, with side boundaries connected to an infinite water aquifer, implying outflow boundary conditions; (b) H₂ is injected at the maximum allowable injection pressure and withdrawn at the minimum allowable production pressure; (c) The gas dissolution is neglected due to a small percentage of dissolved gas compared to free gas [23, 24, 28, 36]; (d) H₂ leakage through the caprock is deemed negligible, thus excluding the caprock from the simulation domain; (e) The diffusion effect is neglected due to its minimal impact on H₂ transport in storage formations with high porosity and permeability, where advection dominates [16, 17, 23, 37].

The simulation domain, illustrated in Fig.1, is used for both saline aquifers and depleted gas reservoirs, measuring 45 km by 45 km in area with a variable thickness of 10 to 300 m. Gas injection and withdrawal occur via the central well. The domain's computational mesh consists of 151 × 151 × 10 grids in the x, y, and z directions, respectively. No-flow boundary conditions apply to the top and bottom surfaces, while the lateral sides allow for outflow. Two sets of initial conditions are required for the two types of formations: saline aquifers require initial reservoir pressure and temperature, and depleted gas reservoirs need these plus initial water saturation (S_w), varying from 0.2 to 0.9. It is assumed that the depleted gas reservoir retains

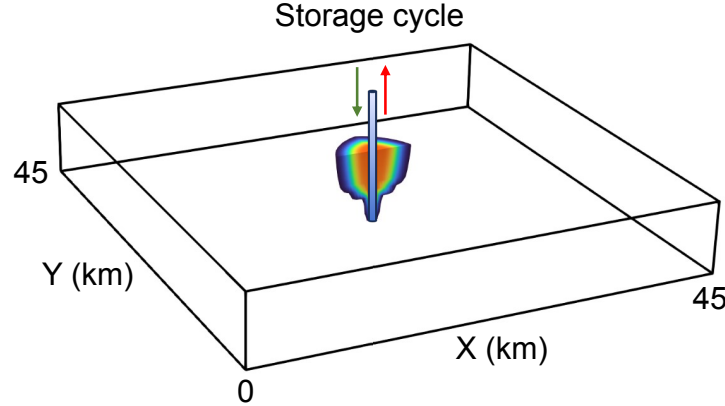


Figure 1: Schematic of simulation domain and well configuration. The well for gas injection and withdrawal is located at the center of the reservoir.

initial or leftover CH₄, with the CH₄ saturation (S_{CH_4}) being calculated as $S_{CH_4} = 1 - S_w$. The initial reservoir pressure is calculated as hydrostatic pressure, and the initial temperature is calculated based on the reservoir depth and geothermal gradient, both of which are geological variables in this study. The relative permeability and capillary pressure curves are sourced from [38].

All the simulations have ten storage cycles, each spanning one year and divided equally into a six-month injection stage and a six-month withdrawal stage. As stated in the assumptions, a constant maximum allowable injection pressure (P_{inj}) for H₂ and cushion gas injection is employed, with its calculation as follows:

$$P_{inj} = P_{litho} \times \alpha \times s_f, \quad (1)$$

where α is the injection pressure coefficient, ranging from 0.6 to 0.8 based on the previous literature [39–41]. s_f denotes a safety factor and equals 0.9 in this study. P_{litho} is the lithostatic pressure determined by [39, 42]

$$P_{litho} = P_{atm} + [\rho_w \phi + \rho_r (1 - \phi)] \times 9.81 \times D. \quad (2)$$

Here, P_{atm} is the atmospheric pressure (0.101325 MPa). ρ_w and ρ_r denote the densities of water and rock, respectively. ϕ is the reservoir porosity, and D is the reservoir depth.

For the withdrawal stages, we adopt the minimum allowable production pressure to retrieve the H₂ at the highest rate. The production pressure ranges from 3 to 6 MPa in this study to ensure that the fluid can be produced from the reservoir to the surface [23].

In simulations involving cushion gases, we consider three typical types: CH₄, N₂, and CO₂. Prior to H₂ cycling, the cushion gas is injected for a specific duration, which is treated as an operational parameter. This cushion gas injection time varies from 2 to 12 months, representing different volumes of cushion gas.

To quantitatively evaluate UHS performance, we define four important metrics based on simulation results, including H₂ withdrawal efficiency E_h (/), produced H₂ purity P_h (/), produced gas-water ratio GWR (/), and well injectivity J ($m^3/s/MPa$). E_h represents the ratio of recovered to injected H₂ volume (m^3) in each storage cycle. P_h denotes the mole fraction of H₂ in the total produced gas stream. GWR is the ratio of the produced gas volume (m^3) to the produced water volume (m^3). Lastly, J measures the capability of injecting H₂ into a geological formation and is calculated as

$$J = \frac{V_{inj_H_2}}{t_{inj} \times (P_{inj} - \bar{P}_{res})}, \quad (3)$$

where $V_{inj_H_2}$ represents the injected H₂ volume in one injection stage of a storage cycle. t_{inj} is the H₂ injection time and equals 6 months. P_{inj} and \bar{P}_{res} are the injection pressure and average reservoir pressure, respectively.

2.2 ROM Development

Based on the reservoir simulation data, we developed a unified ROM utilizing deep neural networks (DNNs). The ROM takes geological and operational parameters as inputs and outputs UHS metrics. The ROM can provide fast and accurate predictions for the cyclic evolution of four UHS metrics in both saline aquifers and depleted gas reservoirs under four cushion gas scenarios.

We employ Latin Hypercube Sampling (LHS) [43] to generate various realizations of input parameters for reservoir simulations. LHS ensures comprehensive sampling of the uncertainty landscape, allowing the ROM to be robustly developed [44]. Table 2 presents the range of uncertain geological and operational parameters for UHS simulations in saline aquifers and depleted gas reservoirs. The only difference between the two storage formations is the initial water saturation (S_w): S_w is consistently 1 in saline aquifers but ranges from 0.2 to 0.9 in depleted gas reservoirs. For cushion gas cases, the cushion gas injection time varies from 60 to 360 days; in simulations without cushion gas, this time is zero. The uncertain parameters are uniformly distributed in their ranges. Using parameters from Table 2, we conduct eight types of reservoir simulations for UHS operations in both storage formations, considering four cushion gas scenarios: none, CH₄, N₂, and CO₂. For each simulation type, we generate 1000 combinations of uncertain parameters as simulation inputs. In total, we perform 8000 reservoir simulations, each comprising ten storage cycles, to predict the cyclic evolution of four UHS metrics.

We develop the ROM based on the reservoir simulation data. The ROM inputs include geological and

Uncertain Parameters	Saline Aquifer		Depleted Gas Reservoir		Units
	Lower Bound	Upper Bound	Lower Bound	Upper Bound	
Reservoir depth	1000	3500	1000	3500	m
Reservoir thickness	10	300	10	300	m
Permeability	1	1000	1	1000	mD
Porosity	0.05	0.36	0.05	0.36	/
Geothermal gradient	0.015	0.045	0.015	0.045	°C/m
Net-to-gross ratio	0.4	1	0.4	1	/
Injection pressure coefficient	0.6	0.8	0.6	0.8	/
Production pressure	3	6	3	6	MPa
Initial water saturation	1	1	0.2	0.9	/
Cushion gas injection time (for cushion gas cases)	60	360	60	360	Days

Table 2: Uncertain geological and operational parameters for UHS simulations in saline aquifers and depleted gas reservoirs under different cushion gas scenarios.

operational parameters, and the outputs are four UHS metrics. In addition to the ten uncertain parameters in Table 2, the storage cycle and cushion gas type are also incorporated as the 11th and 12th inputs into the ROM, respectively. The storage cycle is an integer cycle index ranging from 1 to 10. The cushion gas type is an integer ranging from 0 to 3, representing four cushion gas scenarios: no cushion gas, CH₄, N₂, and CO₂, respectively. All the inputs are normalized to [0, 1] using Min-Max normalization (Eq.4).

$$\hat{x} = \frac{x - x_{\min}}{x_{\max} - x_{\min}}, \quad (4)$$

where x_{\min} and x_{\max} are the minimum and maximum values of parameter x . \hat{x} is the scaled parameter. For the scaling of outputs, E_h and P_h are also normalized by Min-Max normalization, while GWR and J are normalized by log transform first and then normalized by Min-Max normalization. After the data transformation, we split the data into training, validation, and testing sets, with corresponding percentages of 70%, 15%, and 15%, respectively. The training set is used for the model to learn, the validation set helps in tuning and preventing overfitting, and the testing set provides an unbiased evaluation of the model's performance on unseen data. This data separation ensures accurate measurement of the model's effectiveness and generalizability.

The unified ROM is constructed as a fully connected feed-forward deep neural network (DNN) trained with a back-propagation learning algorithm. As shown in Fig.2, the DNN has an input layer, five hidden

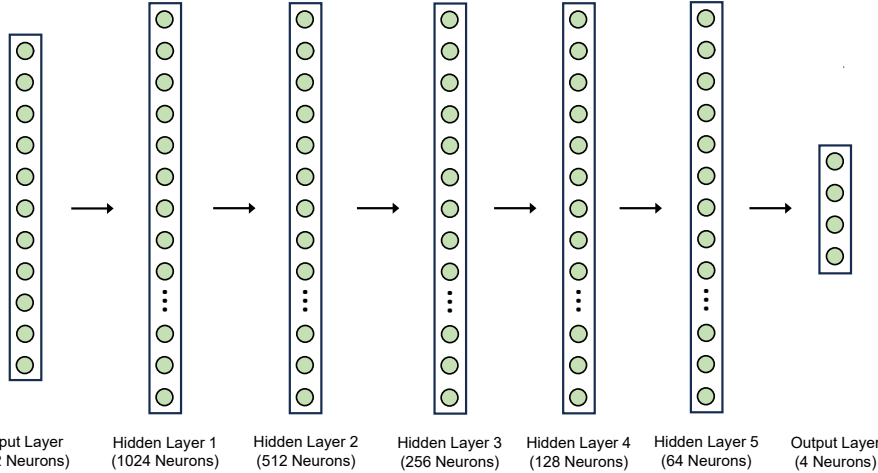


Figure 2: DNN architecture. The DNN has 12 inputs and 4 outputs. The numbers of neurons in the five hidden layers are 1024, 512, 256, 128, and 64, respectively.

layers, and an output layer. The input layer receives 12 inputs, including ten uncertain parameters from Table 2, along with the cushion gas type and cushion gas injection time. The five hidden layers have 1024, 512, 256, 128, and 64 neurons, respectively. In each hidden layer, we perform batch normalization and use the leaky rectified linear units (LeakyReLU) activation function with a negative slope of 0.2. The output layer has 4 neurons, corresponding to the four UHS metrics: E_h , P_h , GWR , and J . The ROM is built using PyTorch [45] and has 714,820 total trainable parameters, namely weights and biases. We train the ROM for 200 epochs using the *Adam* optimizer [46] with a learning rate of 0.002, mean absolute error (MAE) loss, and batch size of 512, which corresponds to approximately 10% of the training data for a total of 10 batches per epoch. These hyper-parameters are selected empirically to maximize the prediction accuracy in the testing set.

3 Results and Analysis

This section comprises four parts: Subsection 3.1 analyzes correlation coefficients among reservoir simulation inputs and outputs. Subsection 3.2 delves into the physical mechanisms of UHS processes, informed by reservoir simulation results. Subsection 3.3 evaluates the ROM performance. Finally, Subsection 3.4 performs an extensive uncertainty quantification for predicting UHS performance in two storage formations under four cushion gas scenarios.

3.1 Correlation Coefficient Analysis

We conducted a correlation coefficient analysis using reservoir simulation data to assess the relationship between simulation inputs (geological and operational parameters) and outputs (UHS metrics). Given our

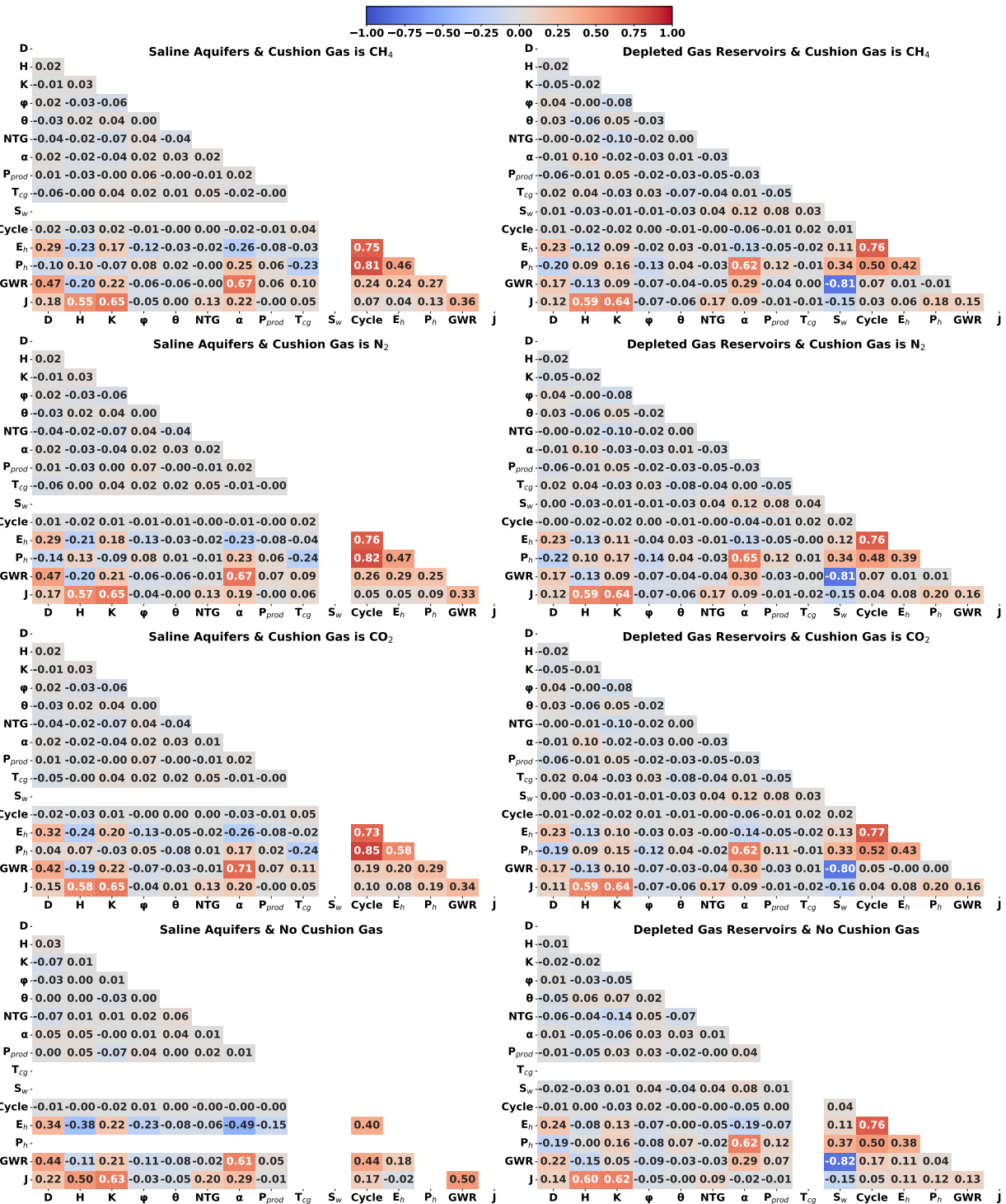


Figure 3: Spearman correlation coefficient matrices for eight types of UHS simulations. The symbols represent: 'D' for depth (m), 'H' for thickness (m), 'K' for permeability (mD), 'ϕ' for porosity (/), 'θ' for geothermal gradient (°C/m), 'NTG' for net-to-gross ratio (/), 'α' for injection pressure coefficient (/), 'P_{prod}' for production pressure (MPa), 'S_w' for initial water saturation (/), 'T_{cg}' for cushion gas injection time (Day), and 'Cycle' for cycle number (/).

1
2
3
4 eight types of UHS simulations across two storage formations and four cushion gas scenarios, we created
5 eight correlation coefficient matrices, each derived from 1000 simulations. These coefficients range from -1 to
6 1, where 1 signifies a perfect positive correlation, -1 indicates a perfect negative correlation, and 0 represents
7 no correlation.
8
9

10
11 As shown in Fig.3, the UHS operations in both saline aquifers and depleted gas reservoirs are technically
12 promising because all the UHS metrics have a positive correlation with the storage cycle, indicating an
13 improving storage performance over cycles. The UHS performance in both formations closely depends on
14 various geological and operational parameters. For instance, E_h in both storage types is strongly positively
15 correlated with reservoir depth, showing that a deeper formation enhances E_h . P_h in both formations posi-
16 tively correlates with the injection pressure coefficient but negatively with reservoir depth. The correlation
17 coefficients for GWR vary significantly. In saline aquifers, GWR is primarily influenced by the depth and
18 injection pressure coefficient, while in depleted gas reservoirs, it is dominated by the initial water satura-
19 tion. In both formations, J positively correlates with reservoir depth, thickness, permeability, and injection
20 pressure coefficient.
21
22

23 In assessing cushion gas effects on UHS performance, we observe that the type of cushion gas has a
24 minimal effect in both formations. This is evidenced by the similarity in coefficient matrices for different
25 types of cushion gases within the same storage formation. However, the influence of cushion gas injection
26 time (T_{cg}) on storage performance varies between the two types of formations. In saline aquifers, T_{cg} exhibits
27 a negative correlation with both E_h and P_h . A longer cushion gas injection (higher cushion gas volume)
28 results in lower H_2 retrievability and purity. Conversely, T_{cg} is positively correlated with GWR and J ,
29 suggesting that increased volumes of cushion gas reduce water production risks and enhance well injectivity.
30 In depleted gas reservoirs, however, the situation differs significantly. The correlation coefficients between T_{cg}
31 and UHS metrics are nearly zero, indicating a negligible impact of cushion gas volume on UHS performance
32 in these reservoirs.
33
34

3.2 Reservoir Simulation Results

35 To understand the physics of UHS processes, we performed eight base cases of reservoir simulations for
36 UHS operations in both saline aquifers and depleted gas reservoirs under four cushion gas scenarios. The
37 input parameters of base cases are the means of parameter ranges. Fig.4 displays the cyclic evolution of
38 the spatial distribution of H_2 saturation of eight base cases. The main observations from the figure are the
39 following:
40
41

- The H_2 plume grows over storage cycles. During injection, the H_2 saturation is high, especially near
the well. During withdrawal, the H_2 saturation drops significantly due to H_2 extraction, but the plume

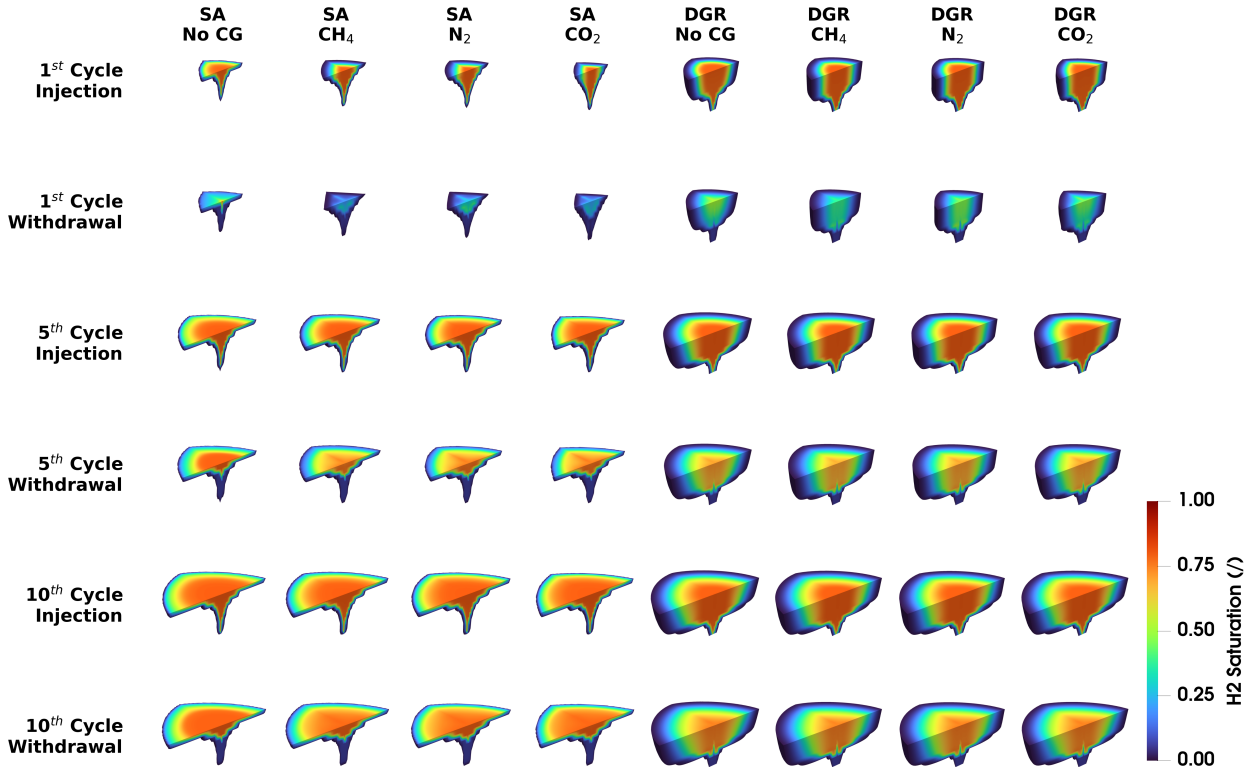


Figure 4: Cyclic evolution of the spatial distribution of H₂ saturation for UHS operations in saline aquifers and depleted gas reservoirs under different cushion gas scenarios (none, CH₄, N₂, and CO₂).

size stays almost the same, indicating that some H₂ remains trapped in the reservoirs. This trapped H₂ amount increases over cycles.

- The shape of the H₂ plume in saline aquifers differs significantly from that in depleted gas reservoirs. In saline aquifers, the H₂ plume, being less dense than water, mostly floats at the reservoir's top due to buoyancy. In contrast, in depleted gas reservoirs, the H₂ plume mixes with the initial CH₄ and migrates deeper into the reservoir. Additionally, the H₂ plume in depleted gas reservoirs is larger than in saline aquifers, suggesting higher well injectivity and greater storage capacity.
- Cushion gas affects H₂ plume migration, but its impact is insignificant. In saline aquifers, cases with cushion gas exhibit lower H₂ saturation near the front of the H₂ plume compared to cases without cushion gas. This lower saturation is attributed to the mixing of H₂ with cushion gas. Additionally, cushion gas injection enhances vertical H₂ plume migration by displacing water from the reservoir top. It also affects the lateral movement of the H₂ plume. Specifically, using CO₂ as a cushion gas restricts the lateral spread of the H₂ plume due to CO₂'s high viscosity. As storage cycles progress, the impact of cushion gas gradually diminishes. In depleted gas reservoirs, cushion gas shows no significant impact throughout all cycles.

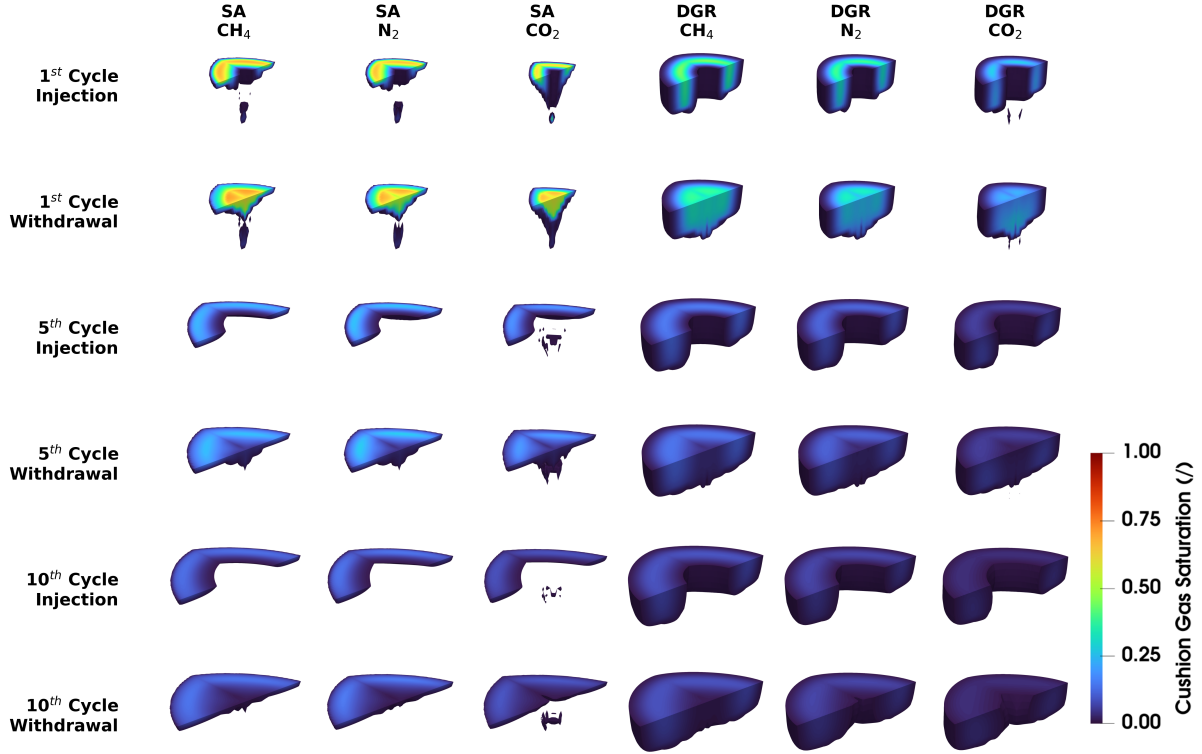


Figure 5: Cyclic evolution of the spatial distribution of cushion gas saturation (CH_4 , N_2 , and CO_2) for UHS operations in saline aquifers and depleted gas reservoirs.

Besides analyzing H_2 plume migration, we also studied the migration of cushion gas plume (Fig.5). The key observations are as follows:

- Under the same injection pressure, saline aquifers receive significantly less cushion gas than depleted gas reservoirs due to their lower well injectivity. In saline aquifers, the cushion gas tends to float atop the formations due to buoyancy. In contrast, in depleted gas reservoirs, the cushion gas plume is much thicker than in saline aquifers, as the densities of the cushion gases are equal to or greater than the initial CH_4 .
- In both formations, cushion gas saturation decreases over cycles, with the cushion gas plume moving away from the well. Initially concentrated near the well, the cushion gas gets pushed further out by the injected H_2 during injection stages. During withdrawal, the cushion gas plume contracts slightly, and some cushion gas is extracted. In both formations, increasing storage cycles lead to more extensive mixing of cushion gas with H_2 and, in the case of depleted fields, with the initial CH_4 as well, resulting in lower cushion gas saturation.
- The migration of cushion gas plumes varies noticeably for different cushion gases. The CO_2 plume, due to its high density, migrates deeper vertically compared to CH_4 and N_2 . Besides density, the viscosity

1
2
3
4 of the cushion gas also influences plume migration. CH₄, with the lowest viscosity among the three
5 gases, forms the largest plume. Note that this low viscosity also facilitates easier CH₄ extraction during
6 withdrawal stages, adversely affecting the purity of the produced H₂. CO₂, having the highest viscosity
7 among the three gases, forms the smallest plume and remains closest to the well.
8
9
10
11
12

13 In addition to analyzing plume migration, we computed the cyclic evolution of UHS metrics for eight
14 base cases. As depicted in Fig.6, UHS shows technical promise in both storage formations, evidenced by
15 improved storage performance over cycles, even without cushion gas. Saline aquifers typically demonstrate
16 higher E_h and P_h but lower GWR and J than depleted gas reservoirs. The impact of cushion gas injection
17 on UHS performance varies between the two formations. In saline aquifers, cushion gas injection drastically
18 reduces E_h and P_h , while significantly enhancing GWR and J . However, in depleted gas reservoirs, cushion
19 gas injection has little impact on E_h , P_h , and J , but notably increases GWR . Note that, in all cushion gas
20 cases, the cushion gas impact is most pronounced in early cycles and diminishes as the cycle increases. The
21 type of cushion gas has a minor effect on storage performance: N₂ slightly outperforms CH₄ and CO₂ in E_h
22 and P_h , while CH₄ excels in terms of J . Regarding GWR , CH₄ is slightly better for depleted gas reservoirs,
23 whereas CO₂ is preferable for saline aquifers.
24
25
26
27
28
29
30
31

32 To further comprehend the underlying physics, we analyzed the cyclic evolution of injected H₂ volume
33 ($V_{inj_H_2}$), produced gas volume (V_{prod_gas}), produced water volume ($V_{prod_H_2O}$), and produced H₂ volume
34 ($V_{prod_H_2}$) for the base cases. As Fig.7a illustrates, under the same injection pressure, depleted gas reservoirs
35 have a much higher $V_{inj_H_2}$ than saline aquifers, indicating a significantly higher H₂ storage capacity. This
36 observation aligns with Fig.4, which shows a larger H₂ plume footprint in depleted gas reservoirs. The high
37 $V_{inj_H_2}$ and the initial CH₄'s high compressibility lead to better well injectivity in depleted gas reservoirs
38 (Fig.6d). Cushion gas injection barely affects $V_{inj_H_2}$ in depleted gas reservoirs but notably enhances $V_{inj_H_2}$
39 in saline aquifers by displacing water from the well, thereby increasing H₂ storage capacity.
40
41
42
43
44
45

46 V_{prod_gas} follows a trend similar to $V_{inj_H_2}$ (Fig.7b). The cushion gas injection significantly increases
47 V_{prod_gas} in saline aquifers. In depleted gas reservoirs, CH₄ as a cushion gas also notably increases V_{prod_gas}
48 in early cycles. However, higher gas production does not always mean higher H₂ recovery. As illustrated in
49 Fig.7c, in saline aquifers, $V_{prod_H_2}$ in cushion gas cases is lower than in the non-cushion gas case at the first
50 cycle, suggesting that much of the early produced gas is cushion gas. Similarly, in depleted gas reservoirs, the
51 CH₄ cushion gas case shows no significant increase in $V_{prod_H_2}$ in the first two cycles, indicating substantial
52 amounts of cushion gas and/or initial CH₄ are produced alongside H₂. The observations from Figs.7b and c
53 elucidate the cyclic evolution of E_h and P_h shown in Fig.6a and b. In saline aquifers, cushion gas injection
54 noticeably increases total gas production but decreases H₂ production in early cycles, thus significantly
55
56
57
58
59
60
61
62

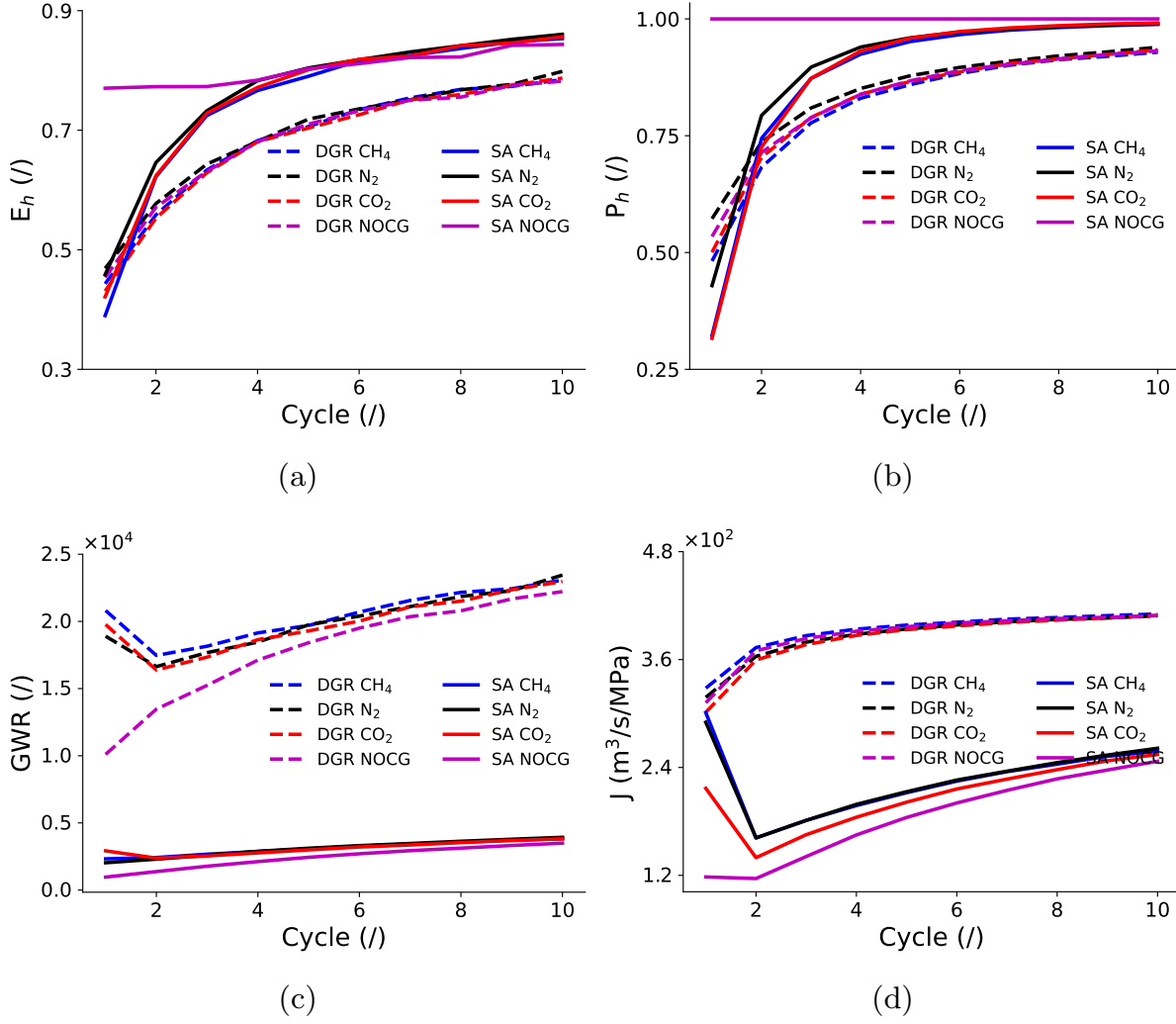


Figure 6: Cyclical evolution of UHS performance metrics for the base cases. (a), (b), (c), and (d) represent the results of E_h , P_h , GWR, and J , respectively.

reducing E_h and P_h . In depleted gas reservoirs, where initial CH_4 is present, cushion gas minimally affects gas production and H_2 recovery, resulting in a lesser effect on E_h and P_h than saline aquifers.

Fig. 7d displays the cyclic evolution of water production for all base cases. As expected, saline aquifers produce more water than depleted gas reservoirs. However, there are similarities in water production across both storage formations. First, without cushion gases, V_{prod-H_2O} decreases over cycles due to increased H_2 trapping during UHS operations, which elevates gas saturation near the well (Fig. 4). Second, cushion gas injection significantly reduces V_{prod-H_2O} in both formations by displacing water from the well. Note that while cushion gases reduce water production in both formations, their impact varies. In saline aquifers, CO_2 outperforms CH_4 and N_2 in reducing water production. Compared to CH_4 and N_2 , CO_2 plume stays closer to the well and migrates deeper along the well (Fig. 5) due to its higher viscosity and density, respectively.

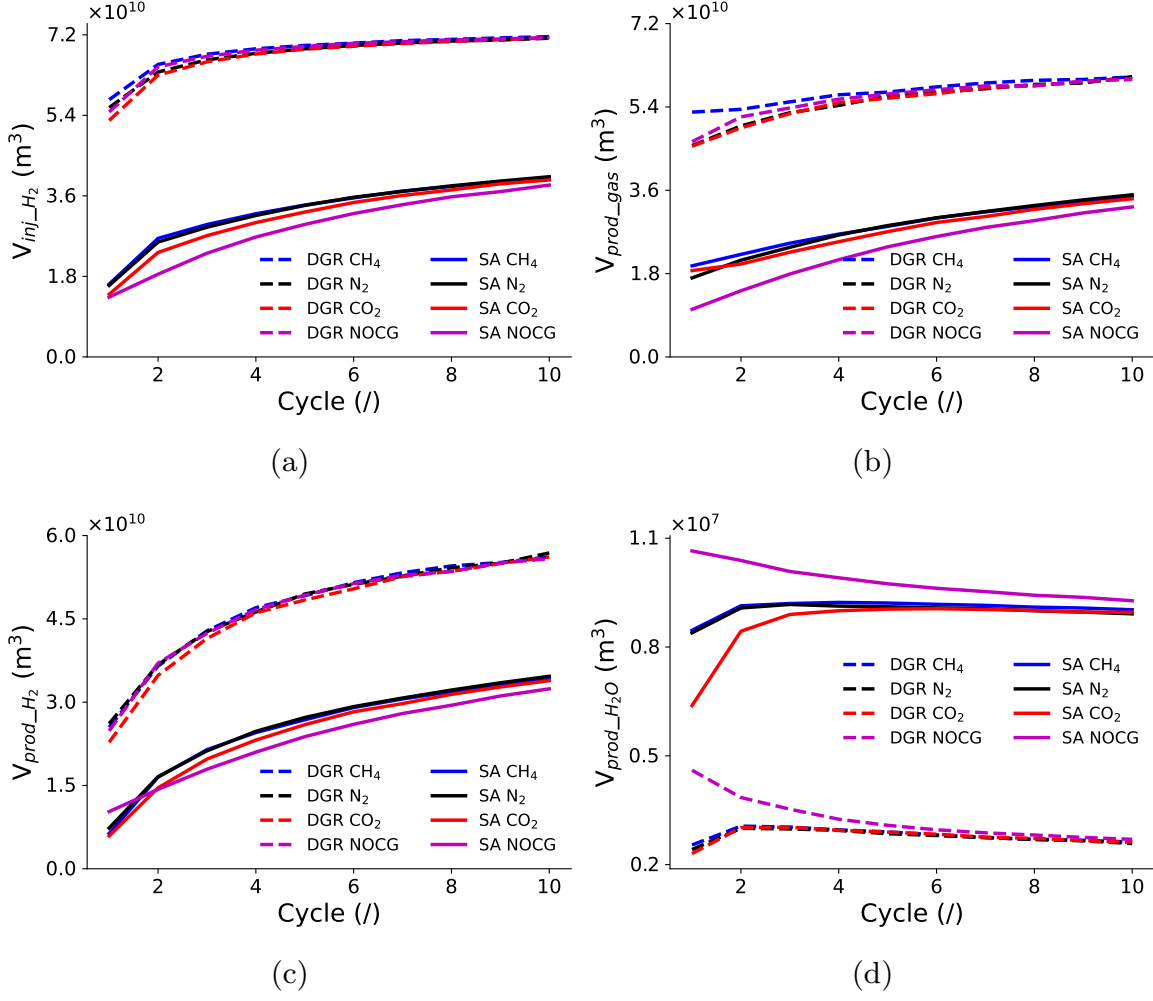


Figure 7: Cyclical evolution of (a) injected H₂ volume, (b) produced gas volume, (c) produced water volume, and (d) produced H₂ volume for the base cases.

The concentrated CO₂ plume near the well effectively mitigates water production, leading to a higher *GWR* (Fig.6c). In contrast, in depleted gas reservoirs, the difference in water production mitigation among various cushion gases is almost negligible. Here, all cushion gas plumes exhibit less gravity override and a larger thickness (Fig.5) due to the presence of initial CH₄, enhancing the sweeping efficiency for water. Therefore, all cushion gases effectively reduce water production in depleted gas reservoirs.

From our previous discussion, we observed that both initial CH₄ and cushion gas can be co-produced with H₂ during withdrawal, negatively impacting E_h and P_h . To quantify the composition of the produced gas stream, we examined the cyclic evolution of the volume fraction of initial CH₄ ($P_{init_CH_4}$) and cushion gas (P_{cg}) in the total produced gas (Fig.8). Fig.8a shows that, in the absence of cushion gas, substantial initial CH₄ is produced in depleted gas reservoirs, with $P_{init_CH_4}$ around 0.5 at the first storage cycle. As the cycle advances, $P_{init_CH_4}$ gradually decreases because the increasing volume of trapped H₂ displaces

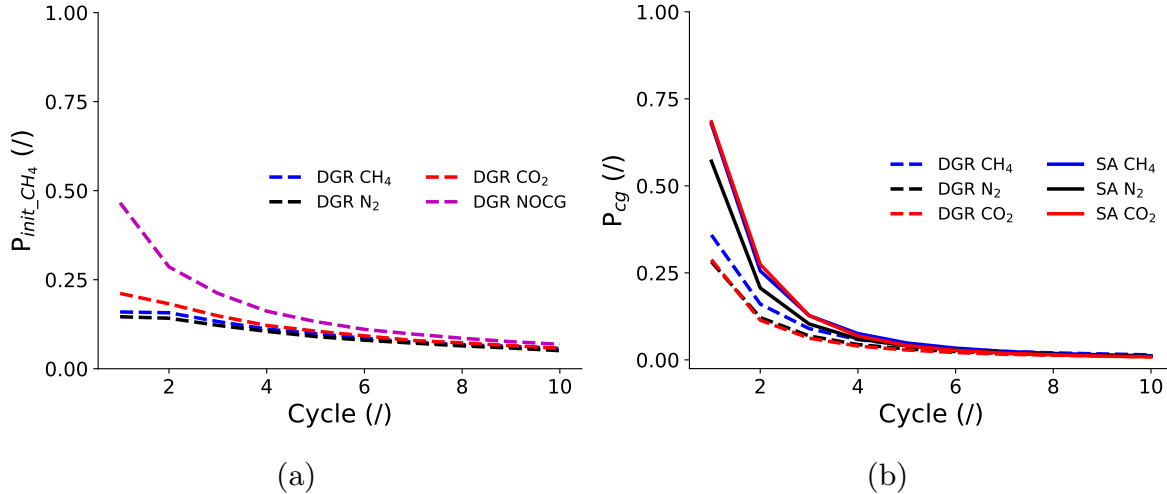


Figure 8: Cyclic evolution of the volume fraction of initial CH₄ (a) and cushion gases (b) in the produced gas stream. The sum of P_h , $P_{init_CH_4}$, and P_{cg} equals 1. To distinguish cushion gas CH₄ from initial CH₄, the cushion gas CH₄ is set as a different component from the initial CH₄ in the DGR CH₄ case, but they have the same properties.

initial CH₄ from the well. Injecting cushion gas significantly reduces $P_{init_CH_4}$ to below 0.25 by effectively sweeping initial CH₄ from the well prior to H₂ cycling. Fig.8b depicts the cyclic evolution of P_{cg} , which peaks early and declines as the cycle progresses. The decline of P_{cg} results from (a) the decreasing volume of remaining cushion gas due to production and (b) the displacement of the cushion gas away from the well. Saline aquifers exhibit a much higher P_{cg} than depleted gas reservoirs, indicating that the cushion gas is easier to produce in saline aquifers. This is because the cushion gas is more concentrated near the well in saline aquifers (Fig.5), facilitating its production. The significant cushion gas production in saline aquifers leads to lower E_h and P_h in the early cycles (Fig.6a and b).

3.3 ROM Performance

Based on the comprehensive reservoir simulation data, we developed a unified ROM using DNN to predict the UHS performance metrics in two storage formations under four cushion gas scenarios. As illustrated in Fig.9, the ROM has great accuracy in predicting all the metrics. The ROM achieves high R^2 (≈ 0.99) and low $\bar{\epsilon}_r$ (average relative error < 0.06) values in predicting four metrics. For all the metrics, the R^2 and $\bar{\epsilon}_r$ for training and validation datasets are similar, indicating that there is no overfitting. The R^2 and $\bar{\epsilon}_r$ for testing datasets are also close to those for training and validation datasets, suggesting that the ROM can achieve great accuracy for unseen data.

To evaluate the efficiency and practicality of the unified ROM, we first examined its training time, followed by an analysis of its prediction time compared to traditional physics-based simulations. The ROM is trained on an NVIDIA RTX A5000 GPU for approximately 315 seconds. The trained model is then used

to predict four UHS metrics. The predictions of UHS metrics evolution in ten storage cycles are obtained in approximately 0.007 milliseconds. Since the physics-based reservoir simulation requires about 10 hours to finish one case, the ROM achieves a speedup factor of over 5,000,000, demonstrating great computational efficiency.

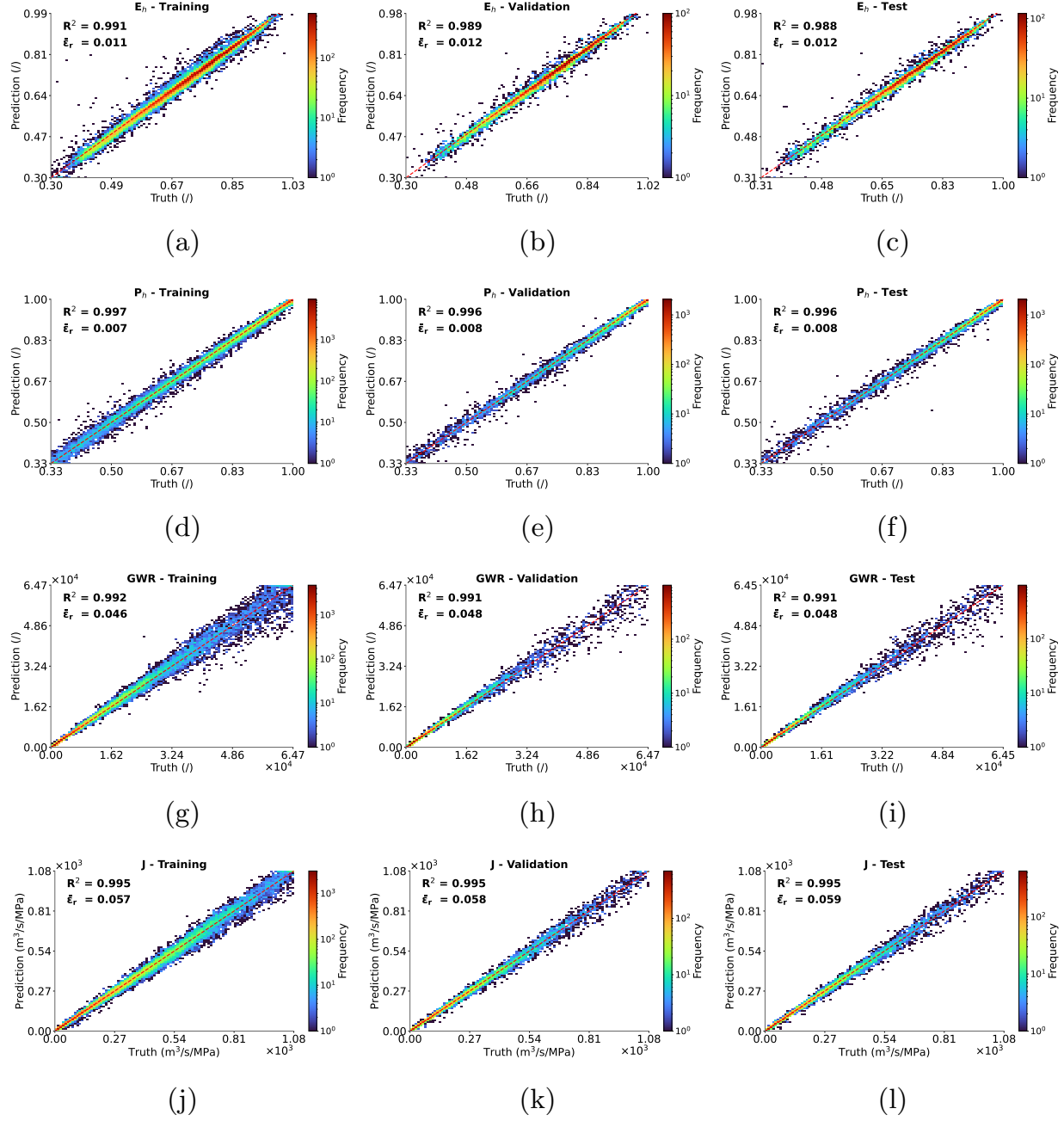


Figure 9: ROM performance for training, validation, and test datasets. A unified ROM has been developed to predict E_h , P_h , GWR , and J simultaneously in two storage formations (saline aquifers and depleted gas reservoirs) under four cushion gas scenarios (none, CH_4 , N_2 , and CO_2). R^2 and $\bar{\epsilon}_r$ (average relative error) values are used to evaluate the ROM performance.

3.5 Uncertainty Quantification

We performed a comprehensive uncertainty quantification for UHS performance prediction using the efficient ROM by varying all the inputs over the entire parameter space. This uncertainty quantification was conducted for two types of formations and four cushion gas scenarios, as depicted in Figs.10 and 11. The ROM generated predictions for 35,328 and 77,824 realizations per storage cycle in saline aquifers and depleted gas reservoirs, respectively, covering four cushion gas scenarios. In Figs.10 and 11, the cyclic evolution of the mean prediction is depicted by the blue line, while the grey area represents the prediction intervals, defined by the P_{10} and P_{90} values. P_{10} refers to the outcome at the 10th percentile, and P_{90} at the 90th percentile, of the cumulative distribution function. Additionally, we computed the average uncertainty (\bar{U}) to further analyze the predictions.

$$\bar{U} = \frac{\sum_{i=1}^n U_i}{n}, \quad (5)$$

$$U_i = P_{90,i} - P_{10,i}. \quad (6)$$

Here, U_i denotes the uncertainty in predicting a specific UHS performance metric at the i^{th} storage cycle. n is the maximum cycle number and equals 10 in this study. The findings from the uncertainty quantification can be divided into two categories.

1. Influence of storage formations on UHS performance

- Saline aquifers show higher E_h compared to depleted gas reservoirs (Figs.10a to d, Figs.11a to d), aligning with the base case observations (Fig.6). The H₂ plume in depleted gas reservoirs has a much larger footprint than in saline aquifers (Fig.4), posing challenges in H₂ recovery. The uncertainty associated with the E_h predictions is slightly higher in saline aquifers.
 - Saline aquifers exhibit higher P_h compared to depleted gas reservoirs (Figs.10e to h, Figs.11e to h). Without cushion gas, P_h in saline aquifers remains around 1.0 throughout the storage cycles. However, upon cushion gas injection, there is a notable decrease in P_h during the early cycles in saline aquifers, though it quickly rebounds to high levels after six cycles. In contrast, depleted gas reservoirs, where H₂ is produced alongside initial CH₄, demonstrate lower P_h . Additionally, the uncertainty in P_h predictions is greater for depleted gas reservoirs than for saline aquifers.
 - Depleted gas reservoirs have a significantly higher GWR compared to saline aquifers, indicating a lower risk of water production (Figs.10i to l, Figs.11i to l). Despite the greater uncertainty in GWR prediction for depleted gas reservoirs, the lower limit of the prediction interval consistently

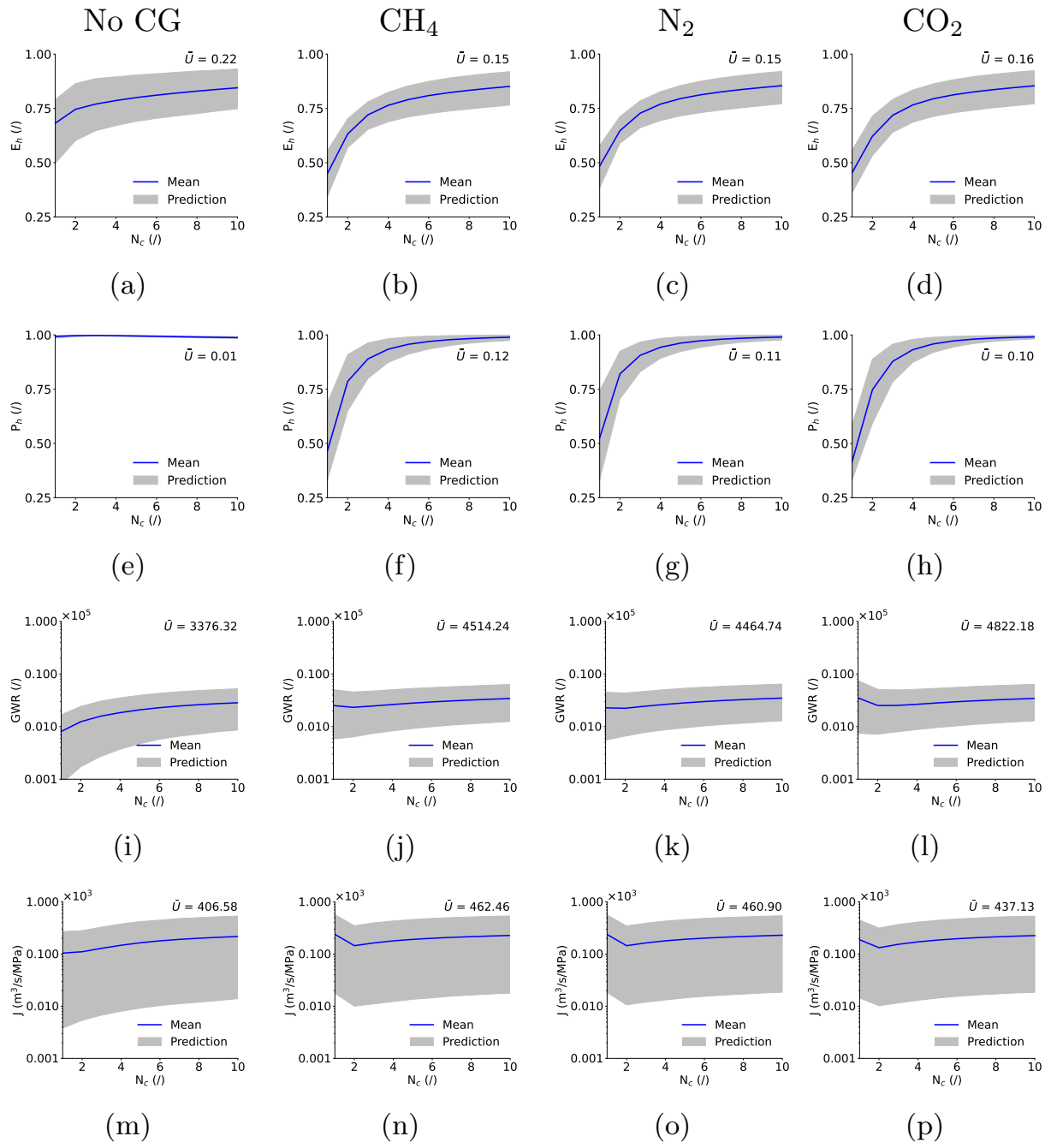


Figure 10: Uncertainty quantification of UHS performance prediction in saline aquifers under four cushion gas scenarios: no cushion gas (a, e, i and m), CH₄ (b, f, j and n), N₂ (c, g, k, and o), CO₂ (d, h, l and p). The blue line represents the mean value of the prediction, and the grey area is the prediction interval from P₁₀ to P₉₀. The \bar{U} is the average uncertainty in the prediction across all the cycles.

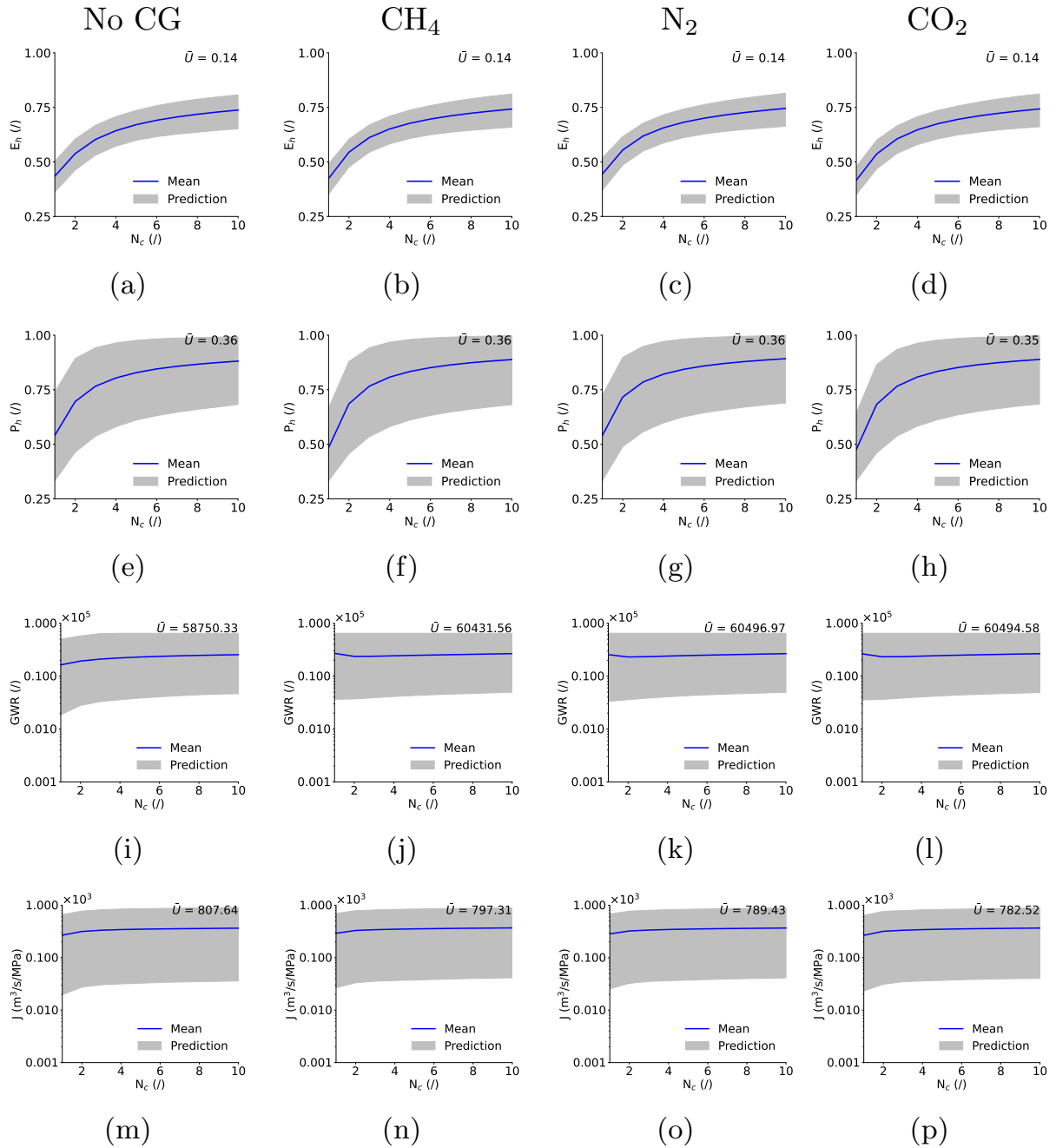


Figure 11: Uncertainty quantification of UHS performance prediction in depleted gas reservoirs under four cushion gas scenarios: no cushion gas (a, e, i and m), CH_4 (b, f, j and n), N_2 (c, g, k, and o), CO_2 (d, h, l and p). The \bar{U} is the average uncertainty in the prediction across all the cycles.

1
2
3
4 exceeds 15,000, indicating minimal water production risks. The lower risk of water production
5 results from the higher gas saturation near the well in depleted gas reservoirs.
6
7

- 8 • Depleted gas reservoirs outperform saline aquifers in J . It is more difficult to inject H_2 into saline
9 aquifers than depleted gas reservoirs due to the much lower compressibility of liquid water than
10 gases. The higher J values in depleted gas reservoirs suggest a greater storage capacity under
11 the same injection pressure, as evidenced by the larger H_2 plume sizes in depleted gas reservoirs
12 (Fig.4).
13
14

15 2. Influence of cushion gas on UHS performance
16
17

- 18 • Cushion gas negatively affects both E_h and P_h in saline aquifers. As observed in base cases, while
19 cushion gas can increase the total volume of produced gas in saline aquifers, it doesn't significantly
20 increase the produced H_2 volume, due to the concurrent production of cushion gas (Fig.7). In
21 the early cycles, a substantial amount of cushion gas is produced, resulting in a marked decrease
22 in both E_h and P_h . However, as the cycles progress, E_h and P_h gradually increase, eventually
23 returning to higher levels in the later cycles.
24
25 • Cushion gas notably enhances GWR and J in saline aquifers, especially in the early storage
26 cycles. As indicated by Fig.10i, some saline aquifers have a high risk of water production, with
27 the lowest GWR less than 100. In such cases, injecting cushion gas prior to H_2 storage is crucial.
28 Cushion gas significantly raises GWR in the early cycles, effectively reducing water production
29 risks. Similarly, cushion gas exerts a strong positive effect on J . As demonstrated in Figs.10m to
30 p, cushion gas greatly improves J in the early cycles by displacing water from the well, thereby
31 enhancing storage capacity under the same injection pressure.
32
33 • Cushion gas has a negligible impact on E_h , P_h , and J in depleted gas reservoirs due to the
34 presence of initial CH_4 (Fig.11). As discussed in base cases, cushion gas injection barely changes
35 the volumes of injected and produced H_2 in depleted gas reservoirs, hence there is little difference
36 in E_h between scenarios with and without cushion gas (Figs.7a and c). Furthermore, since the
37 produced H_2 in depleted gas reservoirs is consistently mixed with initial CH_4 , cushion gas injection
38 has a marginal effect on P_h . Similarly, the inherent high well injectivity in depleted gas reservoirs,
39 driven by the initial CH_4 , means that further improvements in J through cushion gas injection
40 are limited.
41
42 • Cushion gas noticeably enhances GWR in depleted gas reservoirs in the early storage cycles.
43 Compared to saline aquifers, depleted gas reservoirs have a much higher GWR due to a higher
44
45

1
2
3
4 gas saturation near the well. Without cushion gas, the lowest GWR is approximately 16,000 at
5 the first storage cycle. With cushion gas, the lowest GWR increases to around 26,000. However,
6 it's worth noting that while the GWR increase is substantial, the use of cushion gas may not be
7 crucial, as a GWR of 16,000 already suggests a low risk of water production.
8
9

- 10
11
12
13
14
15
16
17
18
19
20
21
22
23
24
25
26
27
28
29
30
31
32
33
34
35
36
37
38
39
40
41
42
43
44
45
46
47
48
49
50
51
52
53
54
55
56
57
58
59
60
61
62
63
64
65
- The cushion gas type has a minor impact on UHS performance. In both formations, N_2 marginally outperforms CH_4 and CO_2 in E_h and P_h . CO_2 slightly excels in GWR , while CH_4 shows a small advantage in J . CH_4 's low viscosity facilitates its easy flow and withdrawal, while CO_2 's high viscosity keeps its plume close to the well, also leading to easier extraction. This ease of withdrawal for CH_4 and CO_2 negatively affects E_h and P_h . In contrast, N_2 , with its moderate viscosity, has the lowest percentage of produced cushion gas in total gas production, yielding the highest E_h and P_h . CO_2 plume, staying close to the well, effectively reduces water contact and enhances GWR . Meanwhile, the extensive spread of the CH_4 plume, due to its low viscosity, positively influences J .
 - Cushion gas has a more substantial impact on UHS performance in saline aquifers than in depleted gas reservoirs. The cushion gas impact is most pronounced in the early storage cycles, diminishing progressively with each cycle and becoming almost negligible after six cycles. In saline aquifers, cushion gas adversely impacts E_h and P_h , yet it markedly enhances GWR and J . In cases where saline aquifers are prone to high water production, the use of cushion gas is recommended to reduce water production risks. In depleted gas reservoirs, under the minimum allowable production pressure, the necessity for cushion gas is reduced due to their inherently high well injectivity and low risks of water production.

4 Conclusions

The study systematically investigates cushion gas effects on UHS performance in porous rocks using reservoir simulation and deep learning. Reservoir simulation provides key insights into the critical physics of UHS operations, while deep learning aids in developing a computationally efficient ROM. This unified ROM allows for extensive system-level analysis of H_2 storage performance in both saline aquifers and depleted gas reservoirs under four cushion gas scenarios: none, CH_4 , N_2 , and CO_2 . Four important UHS metrics (E_h , P_h , GWR , and J) are proposed to quantitatively evaluate H_2 storage performance. Compared to previous literature, this study, for the first time, conducts 8,000 reservoir simulations covering a wide range of geological and operational parameters in potential UHS projects. The extensive reservoir simulation dataset enables a comparative analysis of UHS performance under various reservoir and cushion gas conditions and

1
2
3
4 supports the development of a robust ROM. Remarkably, the ROM is over 5,000,000 times faster than physics-
5 based reservoir simulations, making it ideal for thorough uncertainty quantification in UHS performance
6 prediction. The uncertainty quantification enables a more comprehensive and reliable assessment of H₂
7 storage performance across diverse reservoir and cushion gas conditions. The key conclusions are as follows.
8
9

- 10
11
12 • UHS in porous rocks shows technical promise, as the storage performance improves over cycles, even
13 without the presence of cushion gas. Although UHS metrics may initially start at lower values, they
14 rapidly increase in the early cycles and then steadily stabilize at high levels in the subsequent cycles.
15
16
17 • Saline aquifers exhibit higher E_h and P_h values compared to depleted gas reservoirs. However, they
18 present much lower GWR and J values than depleted gas reservoirs.
19
20
21
22
23 • Cushion gas negatively impacts E_h and P_h in saline aquifers due to the concurrent production of
24 cushion gas with H₂ in the early storage cycles. However, cushion gas significantly improves GWR and
25 J in saline aquifers. Therefore, for saline aquifers at high risk of water production, the use of cushion
26 gas is recommended.
27
28
29
30
31 • Cushion gas is less important in depleted gas reservoirs under the operational conditions of this study,
32 as it has negligible impacts on E_h , P_h , and J . While cushion gas can enhance GWR in the early
33 cycles, its significance is reduced in depleted gas reservoirs, given their inherently low risk of water
34 production.
35
36
37
38 • The cushion gas type slightly impacts UHS performance in both storage formations. N₂ marginally
39 outperforms CH₄ and CO₂ in terms of E_h and P_h . CO₂ is slightly better than other gases in improving
40 GWR , while CH₄ shows a small advantage in enhancing J .
41
42
43
44
45
46
47

48 Declaration of Competing Interest 49

50 The authors declare that they have no competing interests.
51
52

53 54 Acknowledgement 55

56 This work was supported by Los Alamos National Laboratory Technology Evaluation & Demonstration funds
57 and Laboratory Directed Research and Development (LDRD) program.
58
59
60
61
62
63
64
65

References

- [1] Fatih Birol. The future of hydrogen: seizing today's opportunities. *IEA Report prepared for the G 20*, 2019.
- [2] Hassan Nazir, Navaneethan Muthuswamy, Cindrella Louis, Sujin Jose, Jyoti Prakash, Marthe EM Buan, Cristina Flox, Sai Chavan, Xuan Shi, Pertti Kauranen, et al. Is the h2 economy realizable in the foreseeable future? part iii: H2 usage technologies, applications, and challenges and opportunities. *International journal of hydrogen energy*, 45(53):28217–28239, 2020.
- [3] R Tarkowski and B Uliasz-Misiak. Towards underground hydrogen storage: A review of barriers. *Renewable and Sustainable Energy Reviews*, 162:112451, 2022.
- [4] Radoslaw Tarkowski. Underground hydrogen storage: Characteristics and prospects. *Renewable and Sustainable Energy Reviews*, 105:86–94, 5 2019.
- [5] Davood Zivar, Sunil Kumar, and Jalal Foroozesh. Underground hydrogen storage: A comprehensive review. *International Journal of Hydrogen Energy*, 46(45):23436–23462, 7 2021.
- [6] Ahmet Ozarslan. Large-scale hydrogen energy storage in salt caverns. *International Journal of Hydrogen Energy*, 37(19):14265–14277, 10 2012.
- [7] Dilara Gulcin Caglayan, Nikolaus Weber, Heidi U. Heinrichs, Jochen Linßen, Martin Robinius, Peter A. Kukla, and Detlef Stolten. Technical potential of salt caverns for hydrogen storage in Europe. *International Journal of Hydrogen Energy*, 45(11):6793–6805, 2 2020.
- [8] Leszek Lankof, Kazimierz Urbańczyk, and Radosław Tarkowski. Assessment of the potential for underground hydrogen storage in salt domes. *Renewable and Sustainable Energy Reviews*, 160:112309, 5 2022.
- [9] Radosław Tarkowski and Grzegorz Czapowski. Salt domes in Poland – Potential sites for hydrogen storage in caverns. *International Journal of Hydrogen Energy*, 43(46):21414–21427, 11 2018.
- [10] Tao Bai and Pejman Tahmasebi. Coupled hydro-mechanical analysis of seasonal underground hydrogen storage in a saline aquifer. *Journal of Energy Storage*, 50:104308, 6 2022.
- [11] N. Heinemann, J. Scafidi, G. Pickup, E. M. Thaysen, A. Hassanpouryouzband, M. Wilkinson, A. K. Satterley, M. G. Booth, K. Edlmann, and R. S. Haszeldine. Hydrogen storage in saline aquifers: The role of cushion gas for injection and production. *International Journal of Hydrogen Energy*, 46(79):39284–39296, 11 2021.

- [12] Seyed Mostafa Jafari Raad, Yuri Leonenko, and Hassan Hassanzadeh. Hydrogen storage in saline aquifers: Opportunities and challenges. *Renewable and Sustainable Energy Reviews*, 168:112846, 10 2022.
- [13] A. Sainz-Garcia, E. Abarca, V. Rubi, and F. Grandia. Assessment of feasible strategies for seasonal underground hydrogen storage in a saline aquifer. *International Journal of Hydrogen Energy*, 42(26):16657–16666, 6 2017.
- [14] Saeed Harati, Sina Rezaei Gomari, Firdovsi Gasanzade, Sebastian Bauer, Tannaz Pak, and Caroline Orr. Underground hydrogen storage to balance seasonal variations in energy demand: Impact of well configuration on storage performance in deep saline aquifers. *International Journal of Hydrogen Energy*, 4 2023.
- [15] Shihao Wang, Fangxuan Chen, Yu-Shu Wu, and Hadi Nasrabadi. The potential of hydrogen storage in depleted unconventional gas reservoirs: A multiscale modeling study. *International Journal of Hydrogen Energy*, 48(42):16007–16019, 2023.
- [16] Tianjia Huang, George J Moridis, Thomas A Blasingame, Afifi M Abdulkader, and Bicheng Yan. Compositional reservoir simulation of underground hydrogen storage in depleted gas reservoirs. *International Journal of Hydrogen Energy*, 2023.
- [17] Tianjia Huang, George J Moridis, Thomas A Blasingame, Abdulkader M Afifi, and Bicheng Yan. Feasibility analysis of hydrogen storage in depleted natural reservoirs through a multi-phase reservoir simulator. In *SPE Reservoir Characterisation and Simulation Conference and Exhibition*. OnePetro, 2023.
- [18] Lingping Zeng, Mohammad Sarmadivaleh, Ali Saeedi, Yongqiang Chen, Zhiqi Zhong, and Quan Xie. Storage integrity during underground hydrogen storage in depleted gas reservoirs. *Earth-Science Reviews*, page 104625, 2023.
- [19] Nasiru Salahu Muhammed, Md Bashirul Haq, Dhafer Abdullah Al Shehri, Amir Al-Ahmed, Mohammad Mizanur Rahman, Ehsan Zaman, and Stefan Iglauer. Hydrogen storage in depleted gas reservoirs: A comprehensive review. *Fuel*, 337:127032, 2023.
- [20] Esuru Rita Okoroafor, Sarah D Saltzer, and Anthony R Kovscek. Toward underground hydrogen storage in porous media: Reservoir engineering insights. *International Journal of Hydrogen Energy*, 47(79):33781–33802, 2022.

- [21] Reza Ershadnia, Mrityunjay Singh, Saeed Mahmoodpour, Alireza Meyal, Farzad Moeini, Seyyed Abolfazl Hosseini, Daniel Murray Sturmer, Mojdeh Rasoulzadeh, Zhenxue Dai, and Mohamad Reza Soltanian. Impact of geological and operational conditions on underground hydrogen storage. *International Journal of Hydrogen Energy*, 48(4):1450–1471, 1 2023.
- [22] Wolf Tilmann Pfeiffer and Sebastian Bauer. Subsurface porous media hydrogen storage—scenario development and simulation. *Energy Procedia*, 76:565–572, 2015.
- [23] N Heinemann, J Scafidi, Gillian Pickup, EM Thaysen, Aliakbar Hassanpouryouzband, M Wilkinson, AK Satterley, MG Booth, Katriona Edlmann, and RS Haszeldine. Hydrogen storage in saline aquifers: The role of cushion gas for injection and production. *International journal of hydrogen energy*, 46(79):39284–39296, 2021.
- [24] Maojie Chai, Zhangxin Chen, Hossein Nourozieh, and Min Yang. Numerical simulation of large-scale seasonal hydrogen storage in an anticline aquifer: A case study capturing hydrogen interactions and cushion gas injection. *Applied Energy*, 334, 3 2023.
- [25] Qingqi Zhao, Yuhang Wang, and Cheng Chen. Numerical simulation of the impact of different cushion gases on underground hydrogen storage in aquifers based on an experimentally-benchmarked equation-of-state. *International Journal of Hydrogen Energy*, 2023.
- [26] Motaz Saeed and Prashant Jadhawar. Optimizing underground hydrogen storage in aquifers: The impact of cushion gas type. *International Journal of Hydrogen Energy*, 2023.
- [27] Mahdi Kanaani, Behnam Sedaee, and Mojtaba Asadian-Pakfar. Role of cushion gas on underground hydrogen storage in depleted oil reservoirs. *Journal of Energy Storage*, 45:103783, 2022.
- [28] Mohammad Zamehrian and Behnam Sedaee. Underground hydrogen storage in a partially depleted gas condensate reservoir: influence of cushion gas. *Journal of Petroleum Science and Engineering*, 212:110304, 2022.
- [29] Kai Liu, Weiyao Zhu, and Bin Pan. Feasibility of hydrogen storage in depleted shale gas reservoir: A numerical investigation. *Fuel*, 357:129703, 2024.
- [30] Gang Wang, Gillian Elizabeth Pickup, Kenneth Stuart Sorbie, and Eric James Mackay. Driving factors for purity of withdrawn hydrogen: A numerical study of underground hydrogen storage with various cushion gases. In *SPE EuropEC-Europe Energy Conference featured at the 83rd EAGE Annual Conference & Exhibition*. OnePetro, 2022.

- [31] Nasiru Salahu Muhammed, Bashirul Haq, and Dhafer Al Shehri. Co₂ rich cushion gas for hydrogen storage in depleted gas reservoirs: Insight on contact angle and surface tension. *International Journal of Hydrogen Energy*, 2023.
- [32] Nasiru Salahu Muhammed, Bashirul Haq, and Dhafer Al Shehri. Role of methane as a cushion gas for hydrogen storage in depleted gas reservoirs. *International Journal of Hydrogen Energy*, 2023.
- [33] Vahideh Mirchi, Morteza Dejam, Vladimir Alvarado, and Morteza Akbarabadi. Effect of cushion gas on hydrogen/brine flow behavior in oil-wet rocks with application to hydrogen storage in depleted oil and gas reservoirs. *Energy & Fuels*, 37(19):15231–15243, 2023.
- [34] Vahideh Mirchi and Morteza Dejam. Effect of rock surface wettability on hydrogen-cushion gas adsorption with application to hydrogen storage in depleted oil and gas reservoirs. *Journal of Energy Storage*, 73:109152, 2023.
- [35] Rock Flow Dynamics. tNavigator user manual, 2023.
- [36] Raj Kiran, Rajeev Upadhyay, Vinay Kumar Rajak, Saurabh Datta Gupta, and Harharjot Pama. Comprehensive study of the underground hydrogen storage potential in the depleted offshore tapti-gas field. *International Journal of Hydrogen Energy*, 48(33):12396–12409, 2023.
- [37] A Amid, D Mignard, and M Wilkinson. Seasonal storage of hydrogen in a depleted natural gas reservoir. *International journal of hydrogen energy*, 41(12):5549–5558, 2016.
- [38] Sebastian Hogeweg, Gion Strobel, and Birger Hagemann. Benchmark study for the simulation of underground hydrogen storage operations. *Computational Geosciences*, 26(6):1367–1378, 2022.
- [39] Bailian Chen, Dylan R. Harp, Rajesh J. Pawar, Philip H. Stauffer, Hari S. Viswanathan, and Richard S. Middleton. Frankenstein’s ROMster: Avoiding pitfalls of reduced-order model development. *International Journal of Greenhouse Gas Control*, 93, 2 2020.
- [40] Hailin Deng, Philip H. Stauffer, Zhenxue Dai, Zunsheng Jiao, and Ronald C. Surdam. Simulation of industrial-scale CO₂ storage: Multi-scale heterogeneity and its impacts on storage capacity, injectivity and leakage. *International Journal of Greenhouse Gas Control*, 10:397–418, 2012.
- [41] J. Rutqvist, J. Birkholzer, F. Cappa, and C. F. Tsang. Estimating maximum sustainable injection pressure during geological sequestration of CO₂ using coupled fluid flow and geomechanical fault-slip analysis. *Energy Conversion and Management*, 48(6):1798–1807, 6 2007.

- [42] Philip H Stauffer, Hari S Viswanathan, Rajesh J Pawar, and George D Guthrie. A system model for geologic sequestration of carbon dioxide, 2009.
- [43] J. C. Helton and F. J. Davis. Latin hypercube sampling and the propagation of uncertainty in analyses of complex systems. *Reliability Engineering & System Safety*, 81(1):23–69, 7 2003.
- [44] Dylan R. Harp, Rajesh Pawar, J. William Carey, and Carl W. Gable. Reduced order models of transient CO₂ and brine leakage along abandoned wellbores from geologic carbon sequestration reservoirs. *International Journal of Greenhouse Gas Control*, 45:150–162, 2 2016.
- [45] Adam Paszke, Sam Gross, Francisco Massa, Adam Lerer, James Bradbury, Gregory Chanan, Trevor Killeen, Zeming Lin, Natalia Gimelshein, Luca Antiga, et al. Pytorch: An imperative style, high-performance deep learning library. *Advances in neural information processing systems*, 32, 2019.
- [46] Diederik P. Kingma and Jimmy Ba. Adam: A Method for Stochastic Optimization. In *International Conference on Learning Representations*, 12 2014.

Declaration of Interest Statement (use official Word Template)

The authors declare that they have no known competing financial interests or personal relationships that could have appeared to influence the work reported in this paper.